Journal of Materials Chemistry B

Accepted Manuscript

ROYAL SOCIETY OF CHEMISTRY

www.rsc.org/materialsB

The influence of the hydrophilic-lipophilic environment on the structure of silk fibroin protein

Shenzhou Lu[1], Jiaojiao Li[1], Shanshan Zhang[1], Zhuping Yin[1], Tieling Xing[1], David.L.Kaplan[2]
[1]National Engineering Laboratory for Modern Silk, College of Textile and Clothing Engineering, Soochow University, Suzhou 215123, P. R. China
[2] Department of Biomedical Engineering, Tufts University, Medford, MA, 02155, USA

ABSTRACT. The present study examines the influence of the hydrophilic-lipophilic environment, mediated by small molecules, on the structural changes in silk protein fibroin. Small molecules mediate the various hydrophilic-lipophilic balances (HLB) that impact the organisation of silk protein chains. Change in the silk fibroin structure due to additives is related to the HLB value. At HLB >10, the silk fibroin primarily forms Silk I crystalline structures. Small molecules with HLB<8.9 primarily induce the creation of Silk II crystalline structures. When 8.9 < HLB <10, the crystalline structure of the silk is related to the content of the small molecules. The Silk I structure is primarily formed when the content of small molecules is low, whereas the Silk II structure is formed when the small molecule content is high. The structure of the silk fibroin is maintained by regulating the HLB in the fibroin environment. This type of control for the functional design of materials may play a role in fine-tuning the biomaterial properties of silk fibroin protein.

KEYWORDS: silk fibroin; blended film; hydrophilic-lipophilic balances; structure

1. Introduction

Natural protein filaments, such as silkworm silk, exhibit remarkable mechanical performance. The ductility of natural protein filament fibres is higher than most synthetic high-performance fibres [1]. However, the stability mechanism of silk fibroin inside living organisms and the structural changes that occur during silk spinning from solution dope to fibres remain unclear. In particular, upon initial secretion of random coils into the silk gland duct from the epithelial cells, the protein transformation process into periodic β-sheet structures at the spinning end through spinnerets is not fully understood. In silkworms, the concentration of silk protein fibroin in the silk gland reaches above 30 wt% [2]. This exists primarily in the Silk I structure. Simulation of the spinning process *ex vivo* is not able to achieve the same material properties as the silk processed in the native organism. The challenges encountered include the maintenance of high-concentrations of silk solution without the premature formation of β-sheet structures. If β-sheet structures form too early, then spinning becomes problematic. In vivo, such a scenario will obstruct the spinning duct and cause problem for silkworm. The formation of β-sheets prior to spinning limits the ability to spin regenerated silk solutions and obtain fibres with mechanical performance similar to the natural fibres in vitro [3].

Silk protein has been reported to have three crystalline structures: Silk I, Silk II and Silk III [4]. Silk II has an anti-parallel β-sheet structure, Silk I occurs as a metastable state between α-helix and β-sheet structures [5], and Silk III forms at air-liquid interfaces [6]. The metastable Silk I state can exist inside the silk gland even at 30 wt% silk fibroin. Methanol or ethanol facilitates the transformation of silk into Silk II crystalline structures [7, 8]. In our previous investigation, glycerol facilitated silk transformation to Silk I structures [9]. Utilising the different structures, silk fibroin can be used in organic solar cells [10], corneal repair [11], organic conductors [12], drug delivery [13], tissue regenerations [14], and wound healing [15]. Among the three structures, the beta-pleated-sheet crystals of the Silk II structure are the most stable of the protein secondary structures [16]. Why and how can this structure forms from protein solution is very important for understanding the structural changes that occur during the process of preparing silk biomaterials. In addition, elucidating

such mechanisms could help us to better understand Alzheimer's disease due to the secondary protein structural changes to beta-sheets.

Silk fibroin is an amphiphilic polymer with large hydrophobic domains occupying the major component of the polymer, which has a high molecular weight. The hydrophobic regions are interrupted by small hydrophilic spacers, and the N- and C-termini of the chains are also highly hydrophilic [17]. Therefore, the amphiphilicity of the chain organisation likely plays a significant role in relation to the structural state of silk.

The present report examines the mechanism of methanol and glycerol in facilitating the transformation of silk protein fibroin to different structures. To understand such phenomena, small-molecule polyalcohols with different hydrophilic-lipophilic balance (HLB) values are utilised, including butanediol (8.9), propanediol (9.38), ethanediol (9.85), glycerol (11.28), butantetraol (12.7), xylitol (14.13), D-sorbitol (15.55), and inositol (16.74). The HLB values are calculated according to the established protocol [18], and the structural transitions are tracked via FTIR and XRD. Our results precisely describe the transition of the crystalline structure of the silk fibroin protein. This finding may play a role in the design of biomaterials.

2. Materials and Methods

2.1 Preparation of silk fibroin solution

Eighty grams of silk fibre produced by the domestic silkworm, *Bombyx. mori*, were added to 5,000 mL of sodium carbonate solution (concentration: 0.06 wt%), boiled three times at 98−100^{o}C in deionised water, and treated for 30 min each time to remove sericin from the silk fibres. The resulting material was then washed, pulled apart, and dried in a 60^{o}C oven to obtain pure fibroin fibres. These pure fibres were dissolved at 65^{o}C in 9.3 M lithium bromide solution. The ratio of silk to LiBr solution was 1 gram to 15 mL, and the dissolution time was approximately 1 h. After cooling to room temperature, the solution was removed and dialysed in deionised water for 3 d. The dialysed solution was clarified via centrifugation at 4,000 rpm for approximately 30 min. The supernatant, which was an aqueous fibroin

solution, was collected and stored at 4°C. The concentration of this silk solution was approximately 30 mg/mL.

2.2 Preparation of silk fibroin blended films

Polyalcohols were divided into two categories: (1) HLB>10.0, including glycerol, butantetraol, xylitol, D-sorbitol, and inositol; and (2) HLB<10.0, including butanediol, propanediol, and ethanediol. They were prepared in 10% (wt/v) solutions. Aliquots of 40 mL of fibroin solution were added to specific volumes of the polyalcohol solutions to produce polyalcohol/fibroin solutions with the following weight ratios of polyalcohol to silk fibroin: (a) 0 wt%, (b) 10 wt%, (c) 20 wt%, (d) 30 wt%, (e) 40 wt%, (f) 50 wt%, (g) 60 wt% and 100 wt%. After blending, the mixtures were placed in polystyrene plastic moulds and dried in a fume cupboard at room temperature for 10 hours to obtain the blended films.

2.3 Structure of silk fibroin blended films

After the films were prepared, they were processed into very small powders (diameter< 80 μm) using scissors. Subsequently, X-ray diffraction (XRD) was performed using an X-ray diffractometer (X′ Pert-Pro MPD, PANalytical, Almelo, Holland) with CuKα radiation. XRD patterns were recorded at a speed of 10°/min at 40 kv and 35 mA in the region of 2θ from 5° to 45°. The structures of the films were also analysed via Fourier transform infrared spectroscopy (FTIR) using a Nicolet 5700 Fourier transform infrared spectrometer (Nicolet Co., USA) with KBr pellets. The absorbance of the samples at 400−4000 cm^{-1} was measured to obtain the IR absorption spectra of the films.

2.4 Structure of silk fibroin blend solution

The structures of silk fibroin blend solutions were measured via circular dichroism (CD). CD spectra were recorded using a JASCO-815 spectrometer. After mixing the silk solutions with different polyalcohols, the mixtures were loaded in a sandwich quartz cell with a 0.01 mm path length. A wavelength spectrum was recorded between 190 and 240 nm. The

wavelength step was 1.0 nm. Three scans were accumulated and averaged for each spectrum after the background of blank water was subtracted [19].

2.5 Dissolution of silk fibroin blended films

Blended films were cut into approximately 5 mm x 5 mm squares, and one square film was weighed and immersed in ultrapure water in a 2 mL tube to a concentration of 1% (weight of film/volume of water) and incubated at 37ºC for 1 day. After incubation, the dissolved solution was subjected to UV absorbance measurements at 280 nm. The absorbance values were converted to the amount of silk solubilised in water using the purified silk fibroin solution at various concentrations as standards. The amount of dissolved silk fibroin was then compared to the total mass of the film to obtain the percentage of the film dissolved in water.

2.6 Enzymatic degradation of silk fibroin blended films

Protease XIV (from Streptomyces griseus, EC 3.4.24.31, Sigma) was used in our *in vitro* studies of enzymatic degradation. Protease XIV was dissolved in 0.05 M sodium phosphate buffer solution (PBS, pH 7.4) to prepare the enzyme solution (2.0 U/mL). Each sample (50 ± 5 mg, N=3 per time point) of the regenerated silk fibroin blended films was immersed in 5 mL of 2.0-U/mL enzyme solution at 37 ^{o}C. After 1, 3, 6, 9, 12, and 15 days, each solution was replaced with newly prepared solution and collected. Groups of samples were rinsed in deionised water and then dried at 105 ^{o}C to a constant weight. Quantitative change was expressed as the percentage of retention weight divided by the initial dry weight.

3. Results

3.1 Influence of the HLB >10 on the structure of silk fibroin

Several types of polyalcohols with HLB>10, including glycerol, butantetraol, xylitol, D-sorbitol, and inositol, were blended with the silk fibroin and prepared as films by solution casting at room temperature. Subsequently, the influence of the polyalcohol on the structure

of the silk fibroin was determined.

3.1.1 X-ray diffraction

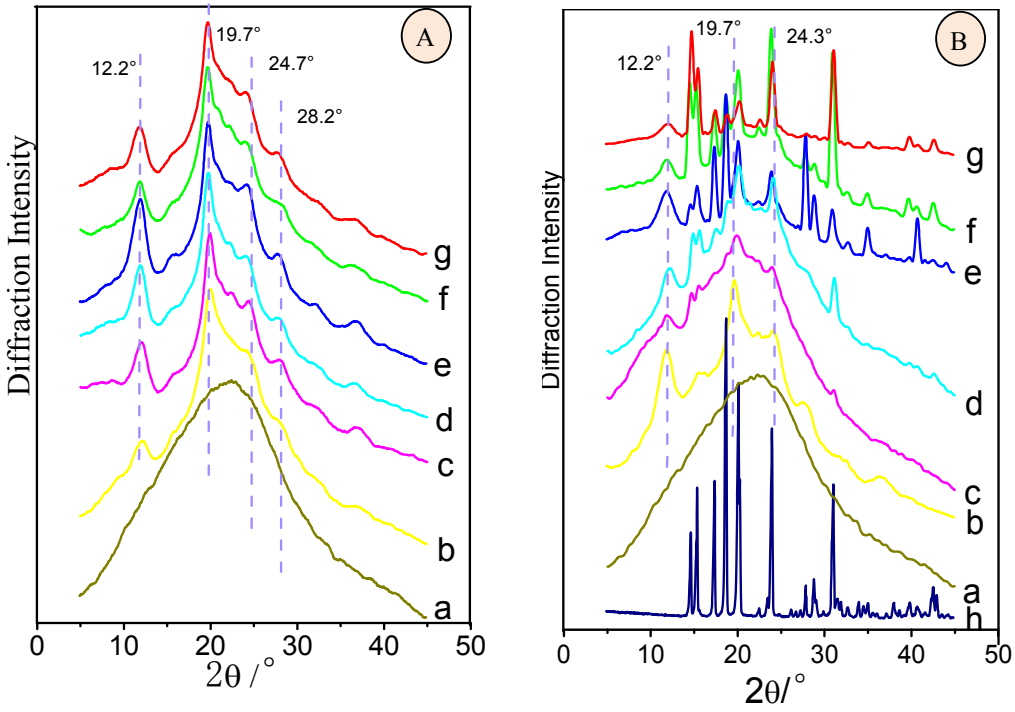

Fig. 1. XRD patterns of polyalcohol/silk fibroin blended films: (A) glycerol, (B) inositol. polyalcohol/silk fibroin ratios= (a) 0 wt%, (b) 10 wt%, (c) 20 wt%, (d) 30 wt%, (e) 40 wt%, (f) 50 wt%, (g) 60 wt%, and (h) pure inositol.

Pure silk fibroin films exhibited a primarily amorphous structure. At a 10 wt% ratio of glycerol/fibroin, the silk exhibited new crystallisation peaks at 2θ=12.2°, 19.7°, 24.7°, 28.2°, and 36.8° (Fig. 1 (A),b), indicating a primarily Silk I crystalline structure [20]. As the content of glycerol was increased, the crystalline structure of the silk remained as Silk I, and no apparent changes were observed. This result indicates that the glycerol facilitates changes in silk fibroin towards a Silk I crystalline structure and not a Silk II structure.

Diffraction peaks of the films of inositol/fibroin=10 wt% appeared at 2θ=12.2°, 19.7°, 24.7°, 28.2°, and 36.8° (Fig. 1(B)). The silk maintained a Silk I structure. When the ratio of inositol/fibroin was increased to 20 wt%, crystallisation peaks of inositol in the blended film appeared at 2θ=14.7°, 15.5°, and 31.2°, and the crystallisation peaks of Silk I at 2θ=12.2°, 19.7°, and 24.7° were still present. When the content of inositol increased, the crystalline

structure of silk in the blended film remained unchanged. The number of crystallisation peaks due to inositol increased, and the peaks became sharper. The diffraction peaks of fibroin at 2θ=19.7° were gradually covered by the diffraction peaks at 2θ=20.1°, indicating that inositol also induced silk transitions from random coils to the Silk I structure. When the ratio of inositol/fibroin exceeded 20 wt%, the inositol in the film began to self-crystallise. Higher contents of inositol induced more apparent crystallisation peaks, indicating poor compatibility or immiscibility between inositol and silk fibroin. Upon addition of butantetraol, xylitol and D-sorbitol, outcomes similar to that of inositol on the silk structure were found. In these cases, the silk fibroin formed Silk I crystalline structures.

3.1.2 FTIR Analysis

As shown in Fig. 2, the FTIR spectra of pure silk fibroin films dried at room temperature have characteristic peaks at 1653.9 cm^{-1} (amide I), 1541.4 cm^{-1} (amide II) and 1237 cm^{-1} (amide III), with fibroin molecules mainly random coils [21]. For glycerol/fibroin of 10 wt%, the position of the absorption peaks remained unchanged for the fibroin molecules in the amide I and amide II regions. The peaks only became wider. Generally, it is difficult to distinguish between random coils and α-helixes via FTIR. Combining the FTIR spectra with the XRD data allowed us to distinguish the conformation of the fibroin as primarily random coils, α-helixes and small amounts of β-sheets. As the content of glycerol increased, the absorption peaks of the blended film at the amide II and amide III regions exhibited no changes, whereas the absorption peaks near 1653 cm^{-1} in the amide I zone sharpened. The results indicate that more fibroin molecules in the blended film were gradually transformed to α-helix as the content of glycerol increased. A new absorption peak appeared near 1525 cm^{-1} in the amide II zone and became apparent when the ratio of glycerol/fibroin exceeded 50 wt%, indicating that the blended film primarily exists as α-helixes even as the content of glycerol is increased.

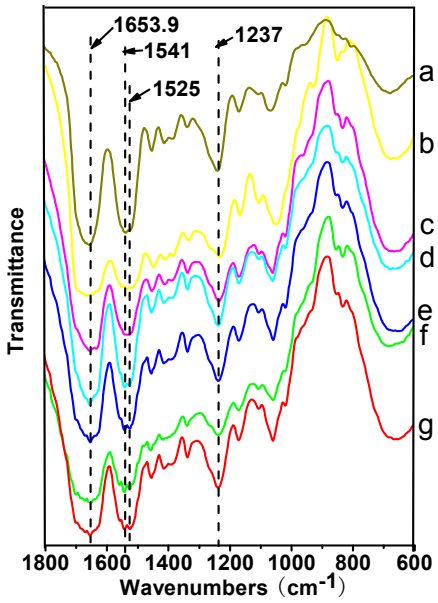

Fig. 2. FTIR of glycerol/silk fibroin blended films.

Glycerol/fibroin ratios= (a) 0 wt%, (b) 10 wt%, (c) 20 wt%, (d) 30 wt%, (e) 40 wt%, (f) 50 wt%, and (g) 60 wt%.

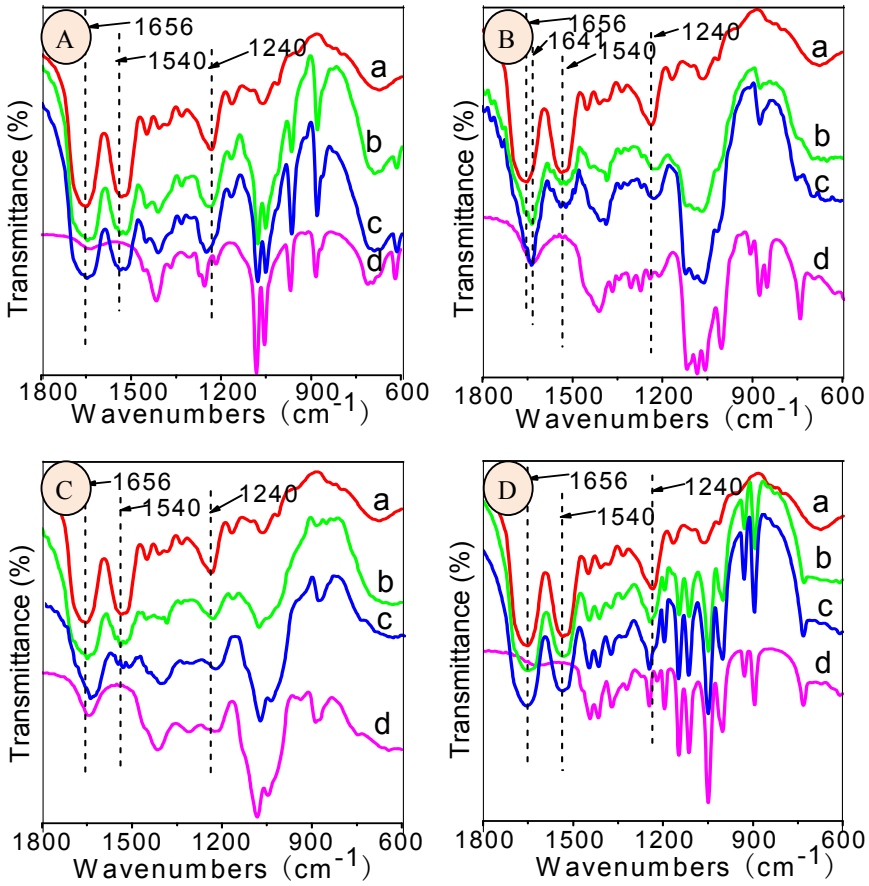

Fig. 3. FTIR of polyalcohol/silk fibroin films. (A) Erythritol, (B) xylitol, (C) D-sorbitol, and (D) inositol. Polyalcohol/silk fibroin ratios = (a) 0 wt%, (b) 30 wt%, (c) 60 wt%, and (d) pure polyalcohol.

As shown in Fig. 3(A), the absorption peaks of the blended film (erythritol/fibroin=30 wt% and 60 wt%) in the amide I and amide II regions appear near 1656 and 1540 cm^{-1}. The absorption peaks in the amide III zone shift toward higher wavelengths in contrast to the pure fibroin membrane. Fibroin in the blended film primarily consisted of α-helical conformations, possibly due to the influence of erythritol. The blended film exhibited four characteristic absorption peaks corresponding to erythritol in the range of 850−1100 cm^{-1}, and the peaks strengthened as the concentration of erythritol was increased. In Fig. 3(B), the blended film (xylitol/fibroin=30 wt%) exhibited two absorption peaks in the amide I zone at 1656 and 1641 cm^{-1}. When the ratio of xylitol/fibroin was increased to 60 wt%, the absorption peak at 1641 cm^{-1} became sharper, and a characteristic absorption peak appeared at 1641 cm^{-1} in the IR spectra of the xylitol crystals. The absorption peak in the amide I zone of the blended film at 1656 cm^{-1} corresponded to fibroin, whereas the peak at 1641 cm^{-1} corresponded to xylitol. As shown in Fig. 3C b and c, the absorption peaks of amide II and amide III were at 1540 and 1240 cm^{-1}. Fibroin in the blended film of xylitol/fibroin primarily formed α-helix structures.

The structures of the D-sorbitol/fibroin and the inositol/fibroin blended films were the same as above discussed. The X-ray diffraction results match the IR spectra well. Polyalcohols with HLB >10 induced the fibroin to form Silk I structures.

3.2 Influence of the HLB < 10 on the structure of silk fibroin

Similarly, different types of polyalcohols with the HLB<10, including butanediol, propanediol, and ethanediol were selected to blend with the silk fibroin. The blended films were fabricated via solution casting at room temperature to determine the influence of the polyalcohols with weak hydrophilicity on the silk protein fibroin structure.

3.2.1 X-ray diffraction

Fig. 4 shows that the pure fibroin membrane primarily exhibited an amorphous structure, whereas the fibroin fibre mainly exhibited a Silk II crystalline structure (2θ=9.1°, 19.7°). The X-ray diffraction curve of the ethanediol/fibroin blended film is shown in Fig. 4(A), which shows the diffraction peaks at 2θ=12.2°, 19.7°, 24.7°, 28.2°, 32.3°, and 36.8° for curves b−f without apparent Silk II diffraction peaks. This result indicates that ethanediol induces fibroin to transform from random coils into Silk I. A weak peak appears at 2θ=9.1° in curve g (Fig. 4(A)), indicating that the fibroin gradually developed a Silk II crystalline structure as the content of ethanediol was increased. Fig. 4(B) shows that the crystallised peaks of fibroin appear at 2θ=12.2° when the ratio of propanediol/fibroin is 10 wt% or 20 wt%, indicating that fibroin under these ratio primarily forms a Silk I crystalline structure. When the ratio of propanediol was increased to 30 wt%, diffraction peaks began to appear at 2θ=9.1° along with the X-ray diffraction curve of the blended film. The crystallised peak at 12.2° becomes weak, and the crystallised peak near 2θ=19.7° shifts to the right to 2θ=20.7°. A crystallised peak appears at 2θ=24.3°, indicating the propanediol/fibroin blended film contains both Silk I and Silk II crystalline structures when the propanediol/fibroin ratio is 30 wt%. Curves e–g. (Fig. 4(B)) reveal that the diffraction peaks of Silk I became weak while those of Silk II gradually strengthened as the ratio of propanediol was increased. The diffraction peak of fibroin exhibited almost entirely the Silk II structure when propanediol/fibroin=60 wt% (Fig. 4(B), curve (g)). Thus, propanediol induced a change in the crystalline structure of fibroin from Silk I at a low ratio to Silk II at a high ratio. The fibroin was present in the Silk II crystalline structure when the ratio of propanediol/fibroin was 60 wt%.

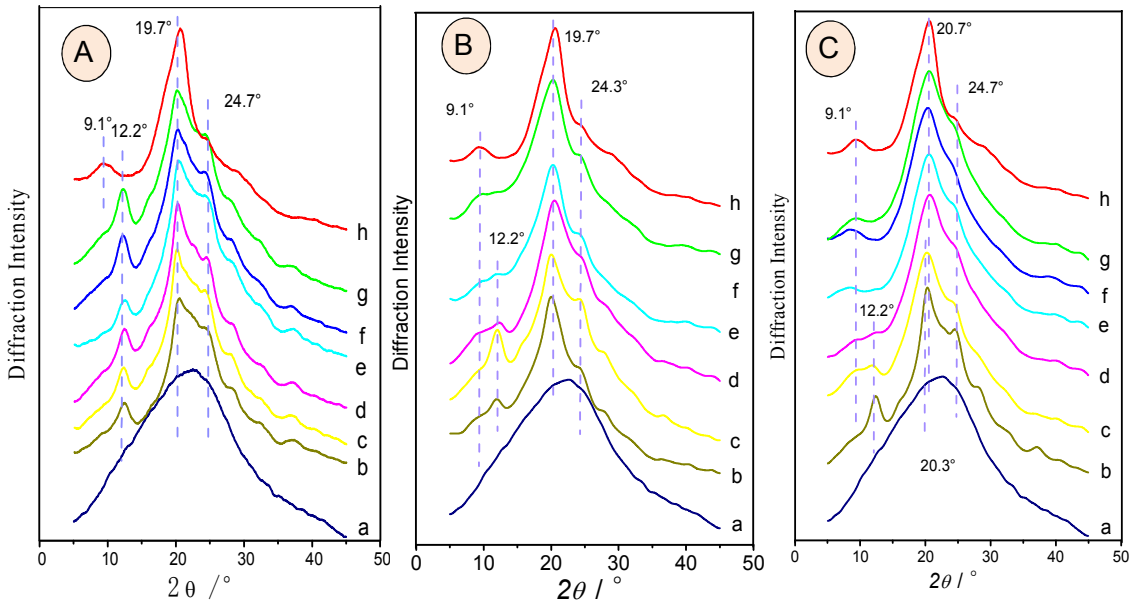

Fig. 4. XRD of dihydric alcohol/silk fibroin blended films. (A) Ethanediol, (B) propanediol, and (C) butanediol. Dihydric alcohol/silk fibroin ratio = (a) 0 wt%, (b) 10 wt%, (c) 20 wt%, (d) 30 wt%, (e) 40 wt%, (f) 50 wt%, (g) 60 wt%, and (h) pure silk fibre.

Fig. 4(C(b)) shows that the diffraction peaks of fibroin appeared at 2θ=12.2°, 19.7°, 24.7°, 28.2°, and 36.8°, indicating a typical Silk I crystalline structure. As the amount of added butanediol was increased, crystallisation peaks appeared at 2θ=9.1° in the X-ray diffraction curve of fibroin. The crystallisation peak at 2θ=19.7° gradually shifted to the right, indicating that fibroin gradually transformed to the Silk II structure when the ratio of butanediol to fibroin was increased. When the ratio of butanediol/fibroin exceeded 40 wt%, the crystallisation peaks of fibroin appeared only at 2θ=9.1°, 20.7°, 24.3°, and 39.7°, indicating a Silk II crystalline structure. The role of butanediol appears to be similar to that of propanediol in fostering a shift to the Silk II structure as the concentration was increased.

3.2.2 FTIR analysis

When ethanediol/fibroin was 10 wt%, 20 wt%, and 30 wt% (Fig. 5(A), curves b–d), the absorption peaks of fibroin in the blended films at the amide I, amide II, and amide III absorption regions were near 1653.8, 1541.9, and 1242 cm^{-1}, respectively. The peaks were

close to the positions of the absorption peaks of pure fibroin membrane. In combination with the X-ray diffraction results described earlier, the fibroin at the three ratios of ethanediol/fibroin blended films exhibited an α-helix conformation. When the ratio of ethanediol/fibroin was 40 wt% and 50 wt% (curves e and f, respectively, in Fig. 5A), the blended films exhibited broader absorption peaks in the amide I and amide II regions. When the ratio of ethanediol was further increased, a new absorption peak gradually appeared at 1629 cm^{-1}, and the absorption peak at 1653.8 cm^{-1} gradually weakened. This result indicates that when ethanediol/fibroin exceeds 40 wt%, the α-helix conformation in the blended film gradually decreases while β-sheet conformation gradually increases. A low proportion of ethanediol facilitated fibroin transformation from a random coil to an α-helix conformation. When the ratio of ethanediol/fibroin was 60 wt%, the fibroin transformed almost entirely to a β-sheet structure with some α-helix structures.

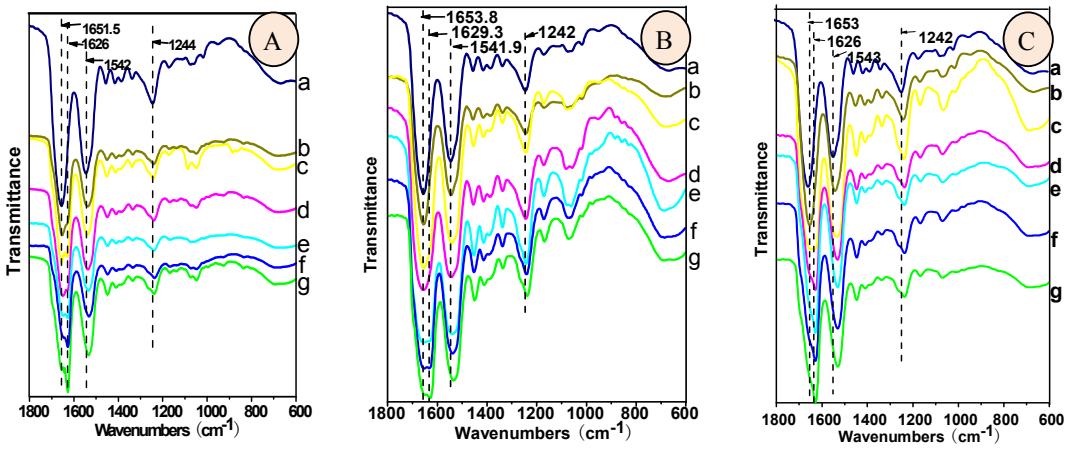

Fig. 5. FTIR of dihydric alcohol/silk fibroin blended films. (A) Ethanediol, (B) propanediol, and (C) butanediol. Dihydric alcohol/silk fibroin ratio = (a) 0 wt%, (b) 10 wt%, (c) 20 wt%, (d) 30 wt%, (e) 40 wt%, (f) 50 wt%, and (g) 60 wt%.

Fig. 5(B) shows that the absorption peaks near 1651 cm^{-1} at the amide I region of the blended films sharpen after the addition of 10 wt% propanediol (curve b). There is a weak absorption peak near 1626 cm^{-1} in the blended film. When combined with the X-ray diffraction results in Fig. 4(B), the data indicate that some random coil structures transform to β-sheet structures. The position of the absorption peaks in the amine II region of curve b in Fig. 5(B) shows no apparent change compared with the pure fibroin membrane. The

absorption peaks in amine III region shifted toward lower wavelengths, similar to the changes in the amide I region. The random coil structures in the fibroin transformed into α-helix conformations when the propanediol/fibroin=10 wt%, and a small amount of β-sheet was also present. When the ratio of propanediol/fibroin was increased to 20 wt%, the absorption peaks of the blended films near 1651 cm^{-1} weakened compared to curve (b). The strengthened peak at 1626 cm^{-1} indicated that a higher ratio of propanediol results in a higher content of β–sheet structures. The main transformation corresponded to random coils converted to α-helixes. As the ratio of propanediol was increased (Fig. 5(B), curves d–f), the absorption peaks near 1651 cm^{-1} gradually weakened until they disappeared. The absorption peaks at 1626 cm^{-1} gradually sharpened due to the continuous addition of propanediol. This facilitates the transformation of random coil structures into β-sheets.

When the ratio of butanediol/fibroin is 10 wt%, the absorption peak in the amide I region of the blended film is 1653 cm^{-1} (Fig. 5(C)), and the peak is sharper than that of the pure fibroin films. The addition of butanediol facilitated the transformation of fibroin from random coils to Silk I. As the ratio of butanediol increased, the absorption peak in the amine I region of the blended film shifted towards lower wavelengths. The absorption peak in the amine I region shifted to 1626 cm^{-1} when butanediol/fibroin=30 wt%, exhibiting β-sheet structures. The absorption peak at 1626 cm^{-1} became sharper as the content of butanediol increased. When the content of butanediol was low, the fibroin transformed from random coils to α-helixes. Butanediol induced fibroin to transform from random coils to β-sheet structures when butanediol/fibroin exceeded 30 wt%.

The influence of polyalcohol with a HLB<10 on the structure of fibroin was different that of butanediol. Ethanediol mainly induced fibroin to transform from random coils to Silk I structures. Silk II structures were obtained only when weight ratios greater than 60 wt% were added. For the propanediol/fibroin blended films, when the ratio of propanediol/fibroin was below 30 wt%, fibroin mainly exhibited a Silk I structure. When the content exceeded 30 wt%, fibroin exhibited a Silk II structure. Butanediol facilitated fibroin to transform more easily into the Silk II structure. When butanediol/fibroin exceeded 20 wt%, fibroin primarily exhibited a Silk II structure. Hence, when the content of polyalcohols with an HLB<10 was low, fibroin transformed from random coils to Silk I structures. The fibroin transformed into

Silk II structures when the polyalcohol content exceeded a critical level. The content of polyalcohol required to facilitate fibroin transformation into different structures was related to the HLB value of the polyalcohol. Smaller HLB values facilitated the transformation to the Silk II structure.

3.3 Structure of silk fibroin blended solution

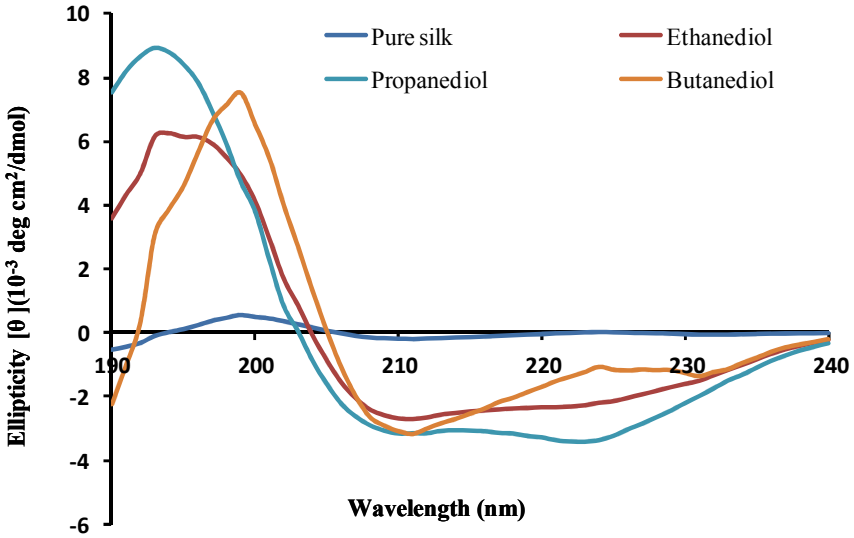

Fig. 6. CD of dihydric alcohol/silk fibroin blended solution

Circular dichroism spectra were recorded after the silk fibroin solution was mixed with various dihydric alcohols, as they induced the fibroin to form different structures (Fig. 6). Pure silk solution showed a low negative Cotton effect at approximately 190 nm with a low positive Cotton effect at approximately 198 nm, which represented typical random coil structures with minimal β-conformation [22]. The SF solutions mixed with different dihydric alcohols resulted in different curves, indicating that SF structure changes during the mixture process. Significant negative Cotton effects at approximately 208 nm and 223 nm with a positive Cotton effect at approximately 195 nm were observed after mixing with ethanediol and propanediol, indicating SF structure changes toward α-helical conformations [23]. In addition, the positive Cotton effect at 195 nm shifted to 198 nm, the negative Cotton effect at approximately 208 nm shifted to 212 nm, and the negative Cotton effect at approximately 223 nm disappeared after butanediol was added into SF solution, which indicated that the SF structure changed to a β-sheet conformation [24].

3.4 Silk fibroin dissolution from blended films

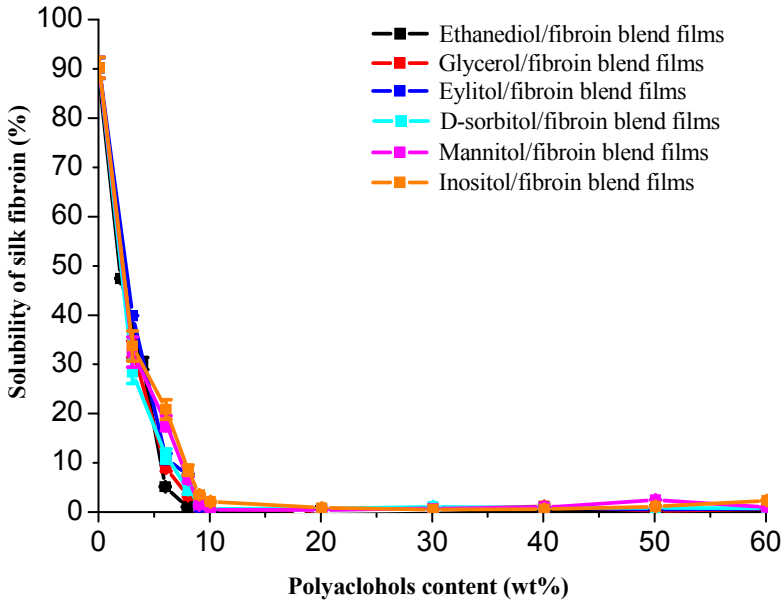

Fig. 7. Dissolution of silk fibroin blended films.

Dissolution of silk fibroin protein from the blended films was determined in water based on the UV absorbance, as silk fibroin protein has a significant tyrosine content that absorbs at 280 nm, whereas glycerol does not absorb at this wavelength. After a rapid initial weight loss at a low content of polyalcohols, no further significant difference was found for the dissolved ratio (Fig. 7). When the polyalcohol content in the blended films was lower than 5 wt%, the solubility of the silk fibroin in the films was higher than 20 %. That indicates that the film could still be dissolved in water. Therefore, polyalcohols at concentrations lower than 5 wt% did not change the resolvability of the silk fibroin in the blended films, as the fibroins maintained random coils. However, when the polyalcohol content in the films was increased to 10 wt%, the solubility of the silk fibroin in the films decreased to less than 2 %. These results indicated that 10 wt% of polyalcohols is a critical concentration for inducing significant changes in the silk film properties, resulting in insolubility of the material in water. Mechanistically, polyalcohols appear to alter the silk fibroin intra- and intermolecular interactions and result in a conformational transition from random coils to Silk I structures or to Silk II structures when the content is more than 10 wt%, as indicated by the above results.

3.5 Enzymatic degradation of silk fibroin blended films

Comparing the influence of the different structures on the degradation of silk fibroin blended films, various dihydric alcohols, ethanediol, propanediol and butanediol, were blended with fibroin to prepare the films. The content of dihydric alcohols was 30 wt%. Under this content, the structure of the ethanediol/fibroin blended films maintained a Silk I structure, the structure of propanediol/fibroin blended films exhibited both Silk I and Silk II structures, and the structure of butanediol/fibroin blended films displayed primarily a Silk II structure. The degradation results of these three dihydric alcohols/silk fibroin blended films compared with pure silk film treated with ethanol (Silk II structure) are shown in Fig. 8.

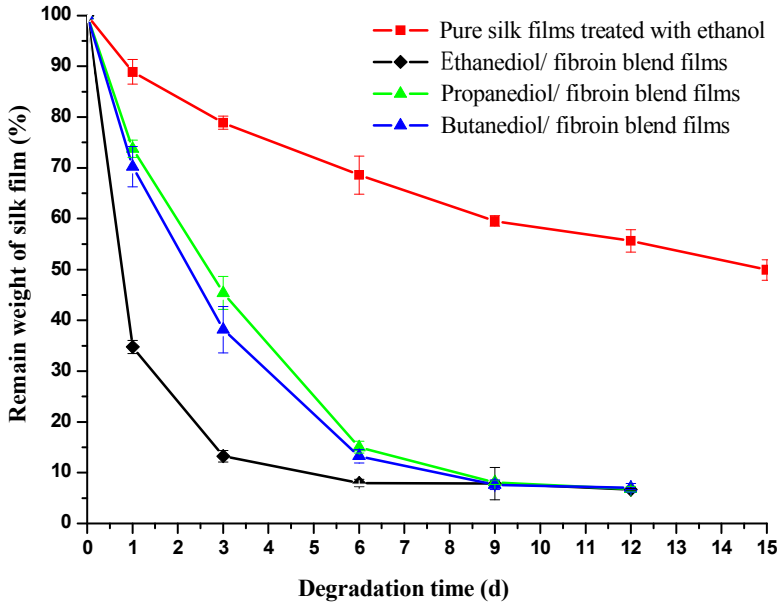

Fig. 8. Quantitative changes of silk fibroin blended films during enzymatic degradation in 2 U/mL protease XIV. The content of dihydric alcohol is 30 wt%.

As shown in Fig. 8, the weights of all of the films decreased within 15 days, which indicated that silk film can be degraded by the enzymes. The degradation rate is very slow for the film treated with ethanol, for which 60 % remained after 15 days of degradation due to the high Silk II crystalline structure. The ethanediol/fibroin blended film degraded very quickly. The weight of the ethanediol/fibroin blended film rapidly decreased, and only 35% remained after just 1 day. The film is almost entirely degraded after 3 days of incubation in

the protease XIV solution. Compared to the ethanediol/fibroin blended film, the other two dihydric alcohols/silk fibroin blended films were slightly degraded. They were almost entirely degraded after immersion in the protease XIV solution for 9 days due to the Silk II crystalline structure in the films because protease XIV can degrade turns but not β-sheet structures [25]. Therefore, the results from Fig. 8 suggest that quantitative changes of the blended films after immersion in enzyme solution depend on the fibroin structure of the films.

4. Discussion

The structure of silk fibroin changes during the process of the silkworm spinning. Studying the environment effects on the silk fibroin conformation will help to elucidate the mechanism of silkworm spinning. The environment of silkworm spinning, including the shearing strength, pH, concentration of metal ions, concentration of the silk fibroins and types of metal ions, were investigated [26]. In this study, we aimed to understand the mechanism of the structure changes due to the hydrophilic-lipophilic environment.

According to previous studies, both methanol (HLB =7.95) [27, 28] and ethanol (HLB=8.43) [29] induce the transformation of fibroin from random coil structures into Silk II structures. In the present study, the use of monohydric, dihydric, and trihydric alcohols resulted in different fibroin structures. Further examination of the physicochemical differences of small-molecule alcohols revealed that increasing the hydrophilicity and hydrophobicity of small-molecule alcohols in the blended film had a remarkable influence on the fibroin structure. The higher the hydrophobicity of the alcohol, the more easily it induced fibroin to transform into a Silk II structure.

Highly hydrophilic alcohols induced fibroin to transform into a Silk I structure. Hence, the relationship between hydrophobicity and Silk I and Silk II structures can be expressed as shown in Fig. 9. When the molecule's HLB>10, fibroin primarily forms a Silk I structure, and when the molecule's HLB<8.5, fibroin primarily transforms a Silk II structure. When the molecule's HLB is between 8.5 and 10, the crystallinity of the fibroin is related to the concentration of molecules in the blended film, mainly developing into a Silk I crystalline

structure when the concentration in the blended film is low. A Silk II crystalline structure forms when the concentration is high.

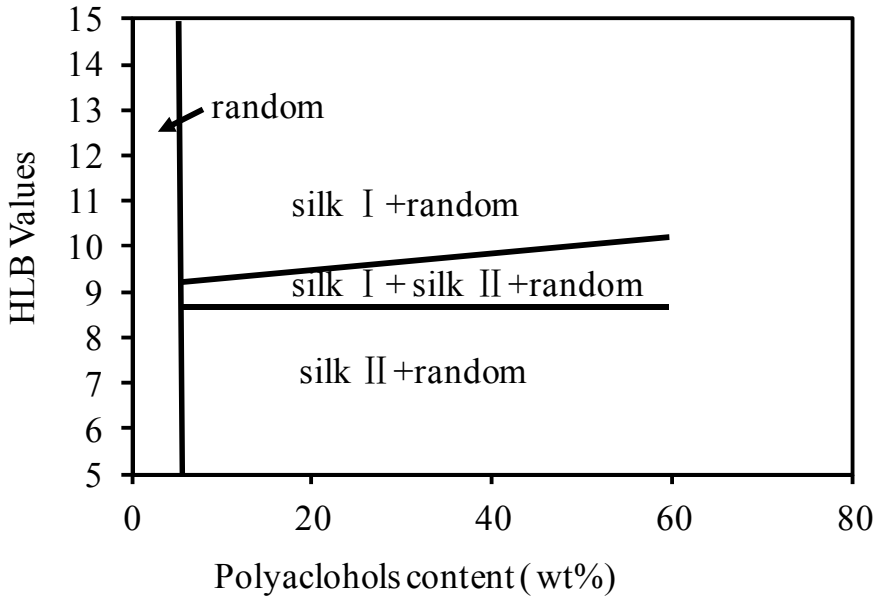

Fig. 9. The effects of the HLB value on the structures of silk fibroin.

The blending of various molecules within silk fibroin has been widely reported. These include polyethylene glycol [30], polyactic acid [31], polyethylene oxide [32], cellulose [33], chitin [34], and polyvinyl alcohol [35]. The fibroin structures in the blended films generally transform from random coil structures to Silk II crystalline structures. Such results conform to the conclusions above concerning the influence of HLB on fibroin structure. To prevent silk fibroin solution gelation, it is important to prevent fibroin transformation from random coils to β-sheet structures. If the fibroin is in an environment with an HLB value >10, the fibroin will transform from random coils to α-helixes, but not to β-sheets. Therefore, some small molecules with high HLB values or salts can be added to the fibroin solution to enhance the hydrophilic environment. Then, the storage time of the liquid silk fibroin will increase, whereas the content of Silk II decreases [36]. This addition will allow fibroin solutions with high concentrations to remain stable prior to and during the spinning process. This procedure will be beneficial for developing nanofiber biomaterials.

5. Conclusions

The influence of polyalcohols with different HLB values, including ethanediol, propanediol, butanediol, glycerol, erythritol, xylitol, D-sorbitol, and inositol, on the fibroin structure was examined. The results revealed that trihydric, tetrahydric, pentahydric, and hexahydric alcohols induce the transformation of silk protein fibroin from random coil structures to Silk I structures. Dihydric alcohols transform fibroin from Silk I to Silk II with increasing alcohol content. The change in the fibroin structure was related to the HLB value of the polyalcohol. When the HLB of the added molecule is >10, fibroin mainly develops a Silk I structure; when HLB<8.5, fibroin primarily develops a Silk II structure; and when 8.5<HLB<10, the crystalline structure of the fibroin is related to the content/stoichiometry of the blended polyalcohols. That is, when the ratio of the polyalcohol added is low, fibroin mainly develops a Silk I structure. When the ratio of polyalcohols added is high, a Silk II structure is formed.

The results indicated that this type of control aid in fine-tuning and engineering the appropriate surface reactions and in providing desirable characteristics of silk fibroin biomaterials for specific applications.

Acknowledement

The work is supported by National Natural Science Foundation of China (Grant No. 51203107, 51373114), PAPD and Nature Science Foundation of Jiangsu, China (Grant No. BK20131176).

References

[1] F. G. Omenetto, D. L. Kaplan, *Science.* 2010, 329(5991), 528-531.
[2] F, Vollrath, D. P. Knight, *Nature.* 2001, 410, 541-548.
[3] H. J. Jin, D. L. Kaplan, *Nature.* 2003, 424, 1057-1061.
[4] O. Kratky, E.Schauenstein, A. Sekora, *Nature.* 1950, 165 (4192), 319-320.
[5] E. S. Sashina, A. M. Bochek, N. P. Novoselov, D. A. Kirichenko, *Russ J. Appl Chem.* 2006, 79(6), 869-876.
[6] R. Valluzzi, S. P. Gido, W. Zhang, W. S. Muller, & D. L. Kaplan, *Macromolecules,* 1996, 29(27),

8606-8614.
[7] M. Tsukada, G. Freddi, P. Monti, A. Bertoluzza, N. Kasai, *J. Polym. Sci. Part B: Polym. Phys.* 1995, 33(14), 1995-2001.
[8] X. Chen, Z. Z. Shao, N. S. Marinkovic, L. M. Miller, P. Zhou, M. R. Chance, *Biophys Chem,* 2001, 89(1), 25-34.
[9] S. Z. Lu, X. Q. Wang, Q. Lu, X. H. Zhang, A. J. Kluge, N. Uppal, F. Omenetto, D. L. Kaplan, *Biomacromolecules.* 2010, 11(1), 143-150.
[10] M. Prosa, A. Sagnella, T. Posati, M. Tessarolo, M. Bolognesi, S. Cavallini, S. Toffanin, V. Benfenati, M. Seri, G. Ruani, M. Muccini, & R. Zamboni, *RSC Advances*, 2014, 4(84), 44815-44822.
[11] J. Wu, J. Rnjak-Kovacina, Y. Du, M. L. Funderburgh, D. L. Kaplan, & J. L. Funderburgh, *Biomaterials,* 2014, 35(12), 3744-3755.
[12] E. Steven, V. Lebedev, E. Laukhina, C. Rovira, V. Laukhin, J. S. Brooks, & J. Veciana, Mater. Horiz, 2014, 1, 522-528.
[13] J. Zhou, B. Zhang, L. Shi, J. Zhong, J. Zhu, J. Yan, P. Wang, C. B. Cao, & D. N. He, *ACS Appl. Mater. Interfaces*, 2014, 6 (24), 21813-21821.
[14] B. Kundu, R. Rajkhowa, S. C. Kundu, & X. Wang, *Adv Drug Deliver Rew,* 2013, 65(4), 457-470.
[15] E. S. Gil, B. Panilaitis, E. Bellas, & D. L. Kaplan, *Adv Healthc Mater*, 2013, 2(1), 206-217.
[16] P. Cebe, X. Hu, D. L. Kaplan, E. Zhuravlev, A. Wurm, D. Arbeiter, & C. Schick, *Sci Rep,* 2013, 3, 1-6.
[17] H. Shulha, C. W. Po Foo, D. L. Kaplan, & V. V. Tsukruk, *Polymer,* 2006, 47(16), 5821-5830.
[18] J. T. Davies, *Proc. Int. Congr. Surface Activ. Lond.* 1957, 426-438.
[19] Y. Yang, Z. Z. Shao, X. Chen, P. Zhou, *Biomacromolecules*, 2004, 5(3): 773-779.
[20] M. Z. Li, S. Z. Lu, Z. Y. Wu, *J. Appl. Polym. Sci.* 2001, 79, 2185-2191.
[21] W. Zhou, X. Chen, Z. Z. Shao, *Prog Chem,* 2006, 18 (11), 1514-1522.
[22] X. Wu, J. Hou, M. Z.Li, J. Wang, D. L. Kaplan & S. Z. Lu, *Acta biomaterialia*, 2012, 8(6): 2185-2192.
[23] K. A. Trabbic, P. Yager, *Macromolecules*, 1998, 31(2): 462-471.
[24] E. Iizuka, & J. T. Yang, *Biochemistry*, 1968, 7(6): 2218-2228
[25] J. Brown, C. L. Lu, J. Coburn, & D. L. Kaplan, *Acta biomaterialia*, 2015, 11: 212-221.
[26] T. Jiang, P. Zhou, *On Biomimetics, Chapter 16*, 2011: 357-372.
[27] N. Minoura, M. Taukada, M. Nagura, *Biomaterials.* 1990, 11(6), 430-434.
[28] E. S. Gil, D. J. Frankowski, M. K. Bowman, A.O. Gozen, S. M. Hudson, R. J. Spontak, *Biomacromolecules.* 2006, 7 (3), 728-735.
[29] Z. B. Cao, X. Chen, J. R. Yao, L. Huang, Z. Z. Shao, *Soft Matter,* 2007, 3, 910-915.
[30] C. X. Liang, H. Kiyoshi, *J. Appl. Polym. Sci.* 1992, 45 (11), 1937-1943.
[31] H. J. Jin, J. Park, R. Valluzzi, P. Cebe, D. L. Kaplan, *Biomacromolecules,* 2004, 5(3), 711-717.
[32] S. Z. Lu, M. Z. Li, Y. Liu, *Polym Mater Sci & Eng.* 2003, 19(1), 104-107.
[33] G. Yang, L. Zhang, Y. G. Liu, *J. Membran Sci.* 2000, 177(1-2), 153-161.
[34] H. Kweon, H. C. Ha, I. C. Um, Y. H. Park, *J. Appl. Polym. Sci.* 2001, (80), 928–934.
[35] T. Tanaka, T. Tanigami, K. Yamaura, *Polym Int.* 1998, 45(2), 175–184.
[36] H. Y. Wang, Y. Q. Zhang, *Soft Matter*, 2013, 9(1), 138-145.